Received: December 19, 2016

International Journal of
Intelligent Engineering & Systems

http://www.inass.org/

Adaptive Fuzzy Logic PI Control for Switched Reluctance Motor Based on Inductance Model

Hady E. Abdel-Maksoud[1*], Mahmoud M. Khater[1], Shaaban M. Shaaban[1]

Faculty of Engineering, Minoufiya University, Egypt
* Corresponding author's Email: hady_elgendy@yahoo.com

Abstract: Aiming to improve the control performance in the switched reluctance (SR) motor drives, this paper presents a simple nonlinear mathematical model of SRM. The model depends on describing the characteristic data obtained from finite element analysis (FEA) in a simple parametric formula. An adaptive fuzzy logic PI controller is used with the suggested model in speed control drive system. The controller is designed based on Mamdani type with nine control rules along with Gaussian function memberships. The control technique is implemented and tested under different operating conditions as well as its results are compared with those of conventional PI controller. Both control schemes operate in pulse width modulation (PWM) control mode. The proposed adaptive fuzzy logic PI improves the motor speed performance in terms of tracking precision and travel time.

Keywords: Switched reluctance motor, PI controller, Adaptive fuzzy logic PI control.

1. Introduction

In recent years, the Switched reluctance motor (SRM) has received considerable attention for the variable speed drive application. It's simple construction due the absence of the magnets, rotor conductors, brushes, and high system efficiency over wide speed range make the SRM drive an interesting alternative to compete with permanent magnet brushless dc motor and induction motor drives. However, the motor has numerous disadvantages due to the motor's doubly salient construction as well as highly pulsating torque output and magnetization characteristics [1, 2]. The advanced control methods can improve the operating performance for the whole motor drive system. However, the highly nonlinear magnetization characteristics of the motor cause that the control of the motor is complicated [3-6]. Earlier control methods can be classified in two groups: those which use a simplified linear model and those which the saturation is taken into account. The simplified linear model schemes have the benefit of simplicity and tractability but are inaccurate in greatest real SR systems, whereas the nonlinear systems have the problem of high complexity and numerical expensiveness which leads to more difficult to represent in real-time [7-13]. A model based on decomposing the magnetic saliencies due to non-uniform air gap and saturation of laminations at high stator currents is proposed [14]. However, the large number of coefficients which should be calculated limit using this model for online control. A nonlinear model of the SRM based on the equivalent magnetic circuit of the motor as a set of reluctances linked in parallel and in series is presented in reference [15]. However, besides, it needs an accurate geometry data; the B-H curve for each part of the machine as well as the magnetization curve should be defined. Some papers proposed an analytical model derived from the motor geometry and material magnetic property [16]. This approach may be useful for the physical machine model; little guidance is given to model the magnetic structure for the purpose of controller design. A piecewise linear

inductance model based on the current and reluctances presented in [17]. The aforementioned discussion concludes that deriving a simple, compact and accurate model to represent the SRM incorporated in a control system is a challenge. In this paper, the FEA is firstly used to analyze the magnetic characteristics of the motor taking the saturation into account. Based on the FEA analysis, a simple nonlinear inductance model is derived. To assure the efficacy of this model in control systems, an adaptive fuzzy logic PI (FLPI) controller is designed. This controller is examined at different transient operations (starting, reference speed change and load change) and compared with conventional PI controller. Both controllers are operated in PWM control mode.

2. The Proposed Model of SRM

The energy conversion principles show that accurate prediction of the SRM developed torque can be obtained from the relationship between the flux linkage (λ), phase current (i) and rotor position angle (θ). These magnetization characteristics can be obtained from direct measurements on an existing motor or alternatively, from sufficiently precise numerical calculations such as finite element analysis (FEA). So, the finite element method FEM is used, firstly, to analyze the magnetic circuit of the motor under study as shown in Fig.1. After that a simplified model is derived based on the results of the FE analysis [18].

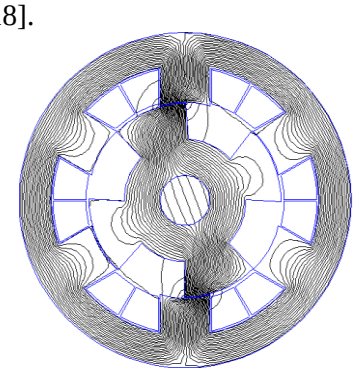

Figure.1 Flux distribution for 3-phase 6/4 SRM

The flux linkage for phase j can be described as:

$$\lambda_j(i_j,\theta) = L_j(i_j,\theta) i_j \quad (1)$$

Where Lj is the self-inductance of phase j. Hence, the self-inductance can be derived from this equation:

$$L_j(i_j,\theta) = \frac{\lambda(i_j,\theta)}{i_j} \quad (2)$$

The self-inductance equation is the key input to the proposed model. Based on the flux linkage and phase current data obtained by FEA, the computer program is built to obtain the self-inductance data as a function i and θ [19]. This data is programmed and simulated to obtain inductance-angle curves at different values of phase current as shown in Fig. 2.

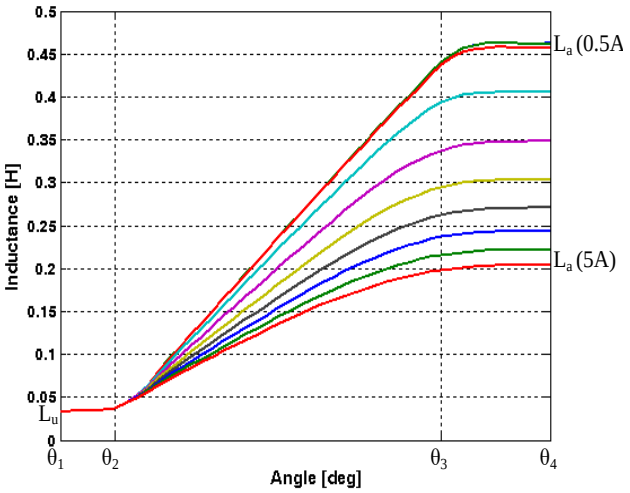

Figure.2 Inductance-angle curves at different values of phase current.

Figure 2 shows the variation of phase inductance versus rotor position angle, from which it can be observed that:

1. The phase inductance is constant from θ1 to θ2 and equal the unaligned inductance value Lu.
2. The phase inductance varies nearly linear from θ2 to θ3 and changes with phase current and rotor position angle.
3. The phase inductance depends only on the phase current from θ3 to θ4 and equal the aligned inductance value La for each value of current.

On the other hand, the phase inductance can be represented by a group of trapezoidal curves; its bottom value is constant at L_u and the top value L_a which changes with phase current. So, it can be described as follows:

$$L_j(i_j,\theta_j) = \begin{cases} L_u & \theta_1 \le \theta \le \theta_2 \\ L_u + k\ \theta_j & \theta_2 \le \theta \le \theta_3 \\ L_a & \theta_3 \le \theta \le \theta_4 \end{cases} \quad (3)$$

$$k = \frac{L_a - L_u}{\beta_S} \quad (4)$$

Where β_S is the stator pole arc, the variation of the aligned phase inductance with the phase current is represented by a second order polynomial equation as

$$L_a = a_0 i_j^2 + a_1 i_j + a_2 \quad (5)$$

The coefficients a0, a1, a2 are determined by the curve fitting method. Based on the formula of the self-inductance L_j, the torque production can be obtained from the basic torque equation:

$$T = \frac{1}{2} i^2 \frac{dL}{d\theta} \tag{6}$$

Substituting Eq. (5) into Eq. (3) one obtains the phase torque as:

$$T_j = \begin{cases} 0 & \theta_1 \le \theta \le \theta_2 \\ \frac{1}{2} i_j^2 \; k & \theta_2 \le \theta \le \theta_3 \\ 0 & \theta_3 \le \theta \le \theta_4 \end{cases} \tag{7}$$

The total developed torque is obtained as the summation of the instantaneous torque developed by all phases.

$$T = \sum_{j=1}^{q} T_j \left(\theta_j, i_j\right) \tag{8}$$

The flux linkage-current characteristics (at aligned and unaligned positions) obtained from the proposed model and from the FEA method are compared. The comparison insures that the curves are typically very close as shown Fig.3.

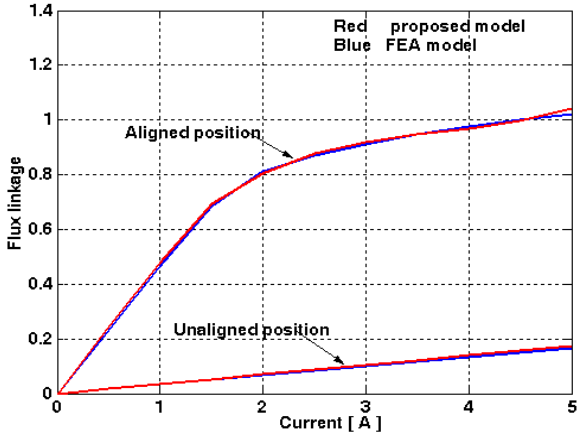

Figure.3 Comparison of flux linkage characteristics for proposed model and FEA

3. Speed Control of SRM

3.1. Conventional PI Controller

With the PI controller, control procedure uses the speed error to determine the reference torque and then determine the reference current which acts with rotor position angle θ and actual currents to produce the commutation angles for hunting the motor to the reference speed command under various operating conditions as shown in Fig. 4.

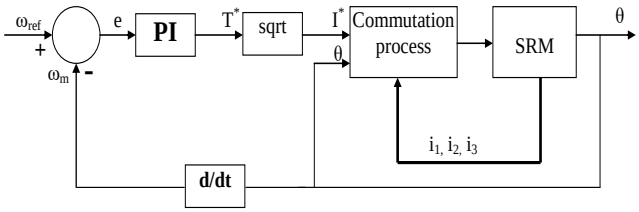

Figure.4 Speed control drive system using PI controller

With the SRM, the proportional integral controller requests to alter its gains with any varying of the operating condition which represents the basic drawback of this controller.

3.2. Adaptive Fuzzy Logic PI Control

If a PI controller be accurately adjusted, the whole control performance will be enhanced and a significant reduction in the overshoot will be obtained. This aim can be gained by designing an appropriate adaptive fuzzy together with PI controller.

Figure 5 shows Block diagram of adaptive fuzzy logic PI controller. The fuzzy controller procedure, in general, is usually sectioned into the following three stages: fuzzification, inference engine and defuzzification. In the fuzzification stage, the real world parameters are converted into fuzzy sets. The control algorithm is coded using fuzzy statements in the block enclosing the information base by taking into consideration the control goals and the system performance. In a fuzzy inference engine, the control actions are coded by means of fuzzy inference rules. The suitable fuzzy sets are realized on the ranges of the involved variables, and fuzzy logic operators and inference methods are modeled in numerical terms. Finally, in the defuzzification block, the results of the fuzzy computations are converted into real values for the fuzzy control action. Each part of FLPI controller system is described in details in the next sections.

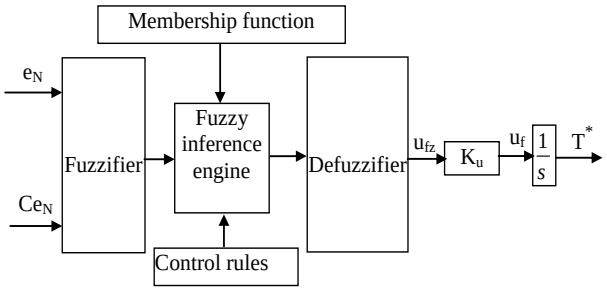

Figure.5 Block diagram of adaptive fuzzy logic PI controller

The overall control system of FLPI along with the SRM is presented in Fig.6.

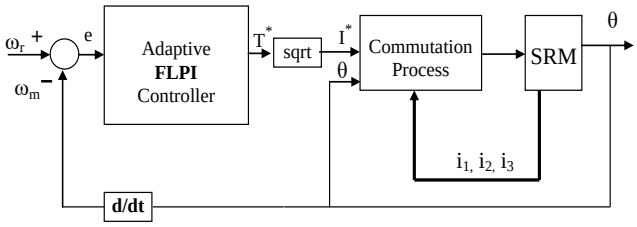

Figure.6 Speed control of SRM using adaptive fuzzy logic PI controller

3.2.1. Input Variables and Normalization

A FLPI controller usually uses the error e(k) and the alteration of error Ce(k) as the input variables:

$$e(k) = \omega_r - \omega_m \tag{9}$$

$$Ce(k) = \frac{e(k) - e(k-1)}{T_s} \tag{10}$$

Where ωr, ωm are required and real motor speeds, respectively, Ts is the sampling time. The input values from the operating domain are first normalized to the range [-1, 1]. Equalization of the inputs e(k) and Ce(k) needs a scale conversion that converts the real values of the system variables into a normalized domain as:

$$e_N(k) = k_e e(k) \tag{11}$$

$$Ce_N(k) = k_d Ce(k) \tag{12}$$

Where k_e and k_d are the input scaling factors.

3.2.2. Membership Functions

In the fuzzification and defuzzification, the membership functions are played an essential role in the final performance of a fuzzy control technique. So, the control effect is strongly depending on the selection of the membership function. Due to its computational efficiency and simplicity, Gaussian function is used with proposed fuzzy logic as shown in Figs. 7, 8.

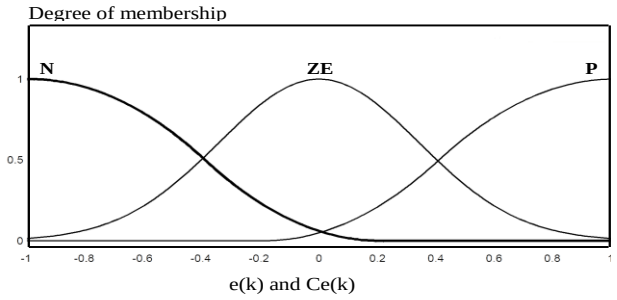

Figure.7 Membership function for error, e(k) and change of error, ce(k)

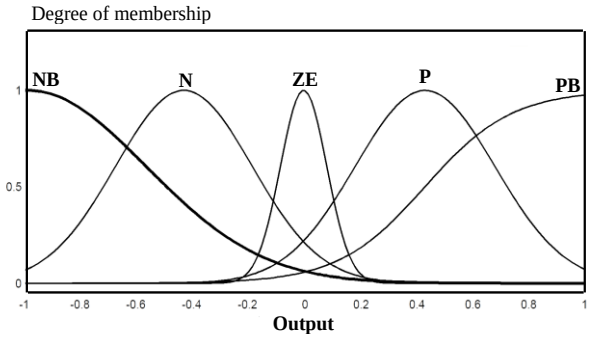

Figure.8 Membership function for the output

3.2.3. Fuzzy Rules

The differential equations are usually used for building the traditional control. However, IF-THEN statements about how to control the system are the language of fuzzy logic control, so an IF-THEN operator is the simplest and mostly used interpretation and, it supplies computational efficiency.

Nine control rules are designed and given in Table 1. Every couple of speed error and speed error change inputs triggers one rule. The Mamdani sort controller is chosen because highly short time is needed for its improvement the simplicity with which its functions can be understood emulated with the Sugeno–Tagaki type controller.

Table.1 The suggest rules for the fuzzy controller

e(k)		N	ZE	P
ce(k)	N	NB	N	P
	ZE	N	ZE	P
	P	ZE	P	PB

3.2.4. Output Normalization

The rules together the membership functions of the fuzzy inputs along with the engine inference, decide the output $u_{fz}(k)$ in the defuzzification. A scaling factor is used to denormalize this output for obtaining the real control input $u_f(k)$:

$$u_f(k) = k_u u_{fz}(k) \tag{13}$$

3.2.5 Pulse Width Modulation Control Mode

The information of both the phase reference currents and the actual ones are treated using the feedback pulse width modulation (PWM) technique with adjusted hysteresis-band which is a function of phase current. The current command is added and

subtracted from the hysteresis window, to obtain the maximum and minimum current values that determine the switching of the phase and main switches of any converter. Figures 9, 10 show the current and voltage waveforms for the SRM under PWM technique.

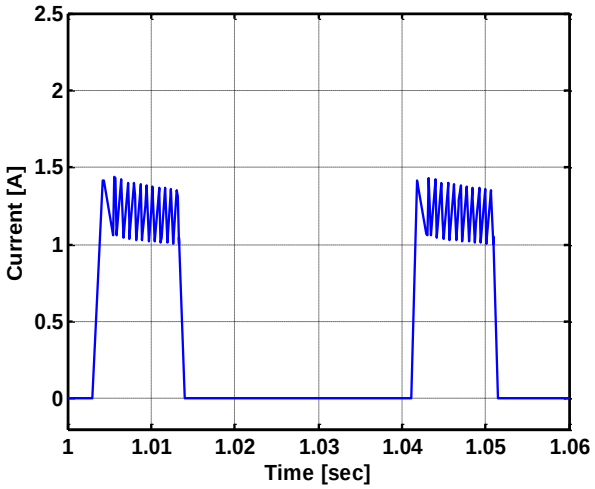

Figure.9 Instantaneous phase current waveform

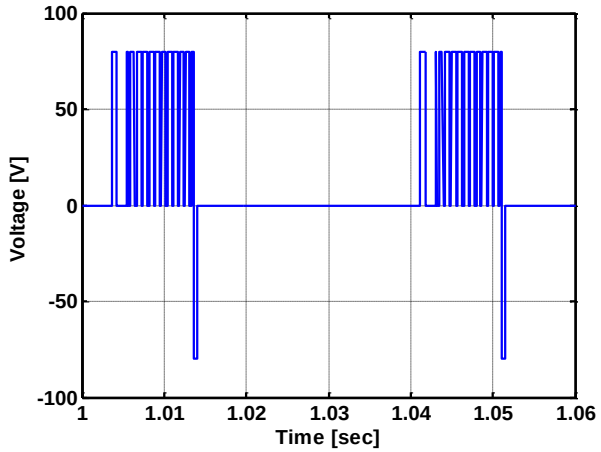

Figure.10 Instantaneous phase voltage waveform

4. Simulation Results

4.1. Starting

In this test the motor is started at rated voltage with a load torque of 0.4 N.m. Figure 11 shows the speed response for the two types of control systems at starting. It is observed that for adaptive FLPI controller, the motor settles after about 0.2 sec with no overshoot while for conventional PI controller, it takes about 0.8 sec with an overshoot about 5%. Figures 12 and 13 show the current and torques responses for the two controllers at starting. The responses of the two controllers are comparable however, the conventional PI demands slightly higher current to overcome its higher torque overshoot.

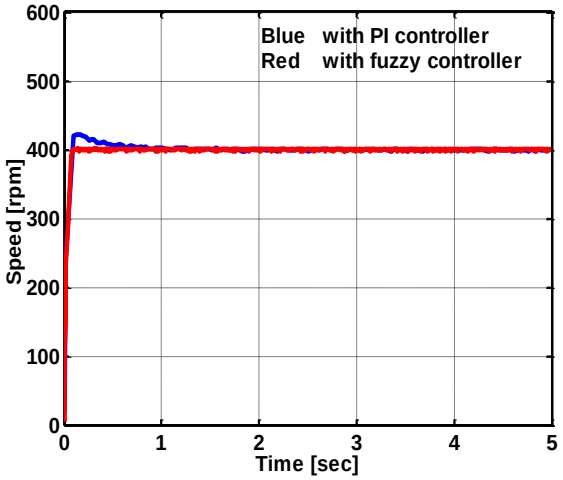

Figure.11 Comparison of the motor speed in the start-up for PI and FLPI controllers.

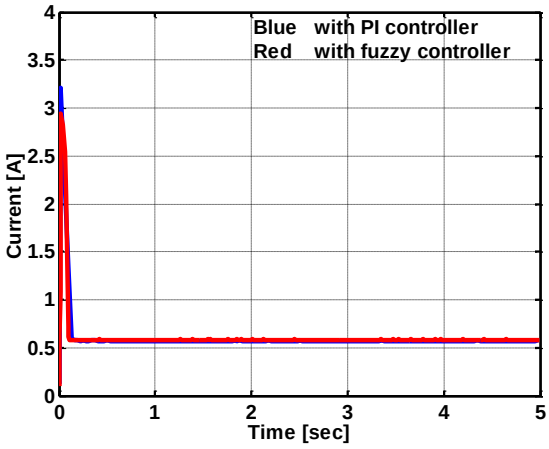

Figure.12 Comparison of the dc link current in the start-up for PI and FLPI controllers.

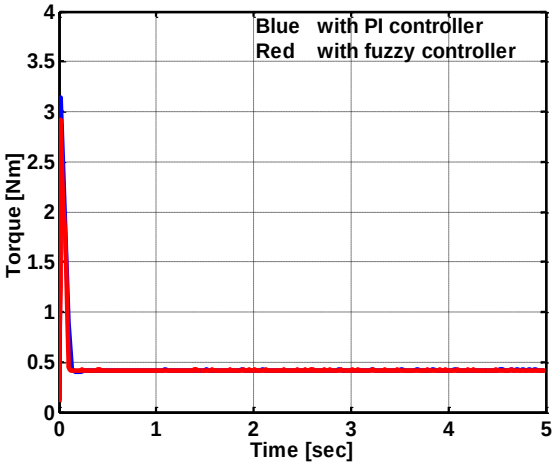

Figure.13 Comparison of the developed torque in the start-up for PI and FLPI controllers.

4.2. Speed change

The motor speed is subjected to a positive and negative step changes by 25%. Figure 14 shows the speed response for positive step change in the speed reference. It is clear that with adaptive FLPI the motor speed settles at the new level faster than conventional PI. The current and torque responses for this condition are shown in figures 15 and 16. It is observed that adaptive FLPI has a more bounded response.

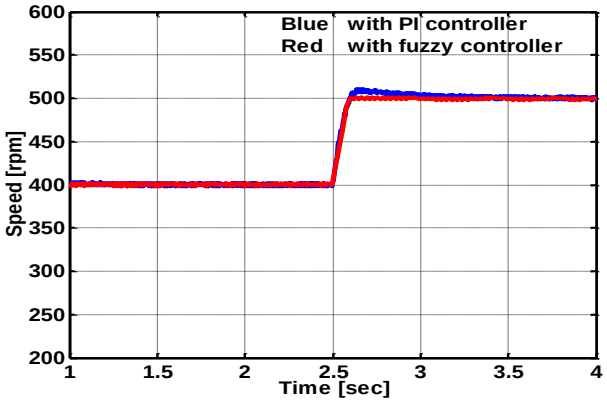

Figure.14 Comparison of the motor speed with positive change in reference speed for PI and FLPI controllers

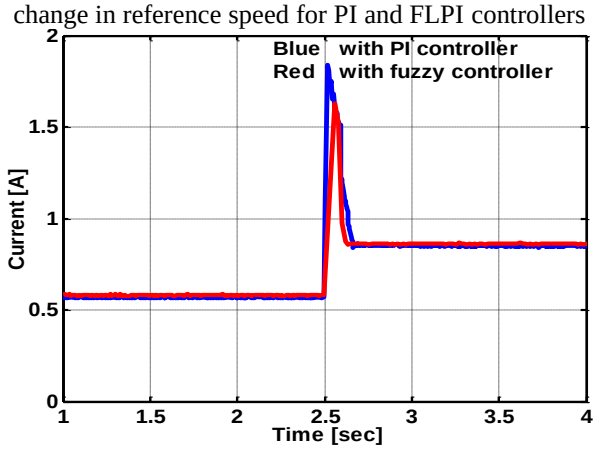

Figure.15 Comparison of the dc link current with positive change in reference speed for PI and FLPI controllers.

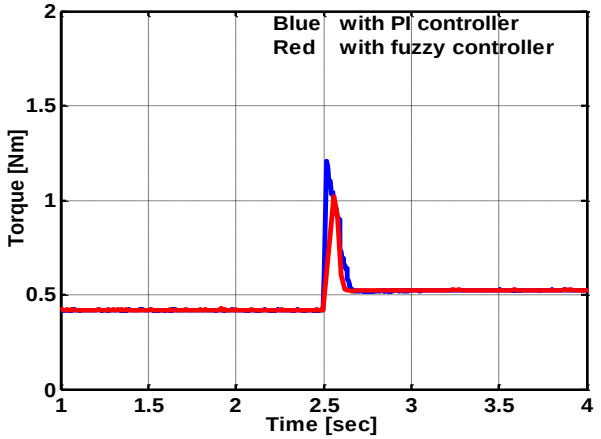

Figure.16 Comparison of the developed torque with positive change in reference speed for PI and FLPI controllers.

Figures 17, 18 and 19 show the speed, current and torque responses for negative step change in the speed reference. The close observation of these figures shows that, similar to positive step change, the adaptive FLPI has a better response.

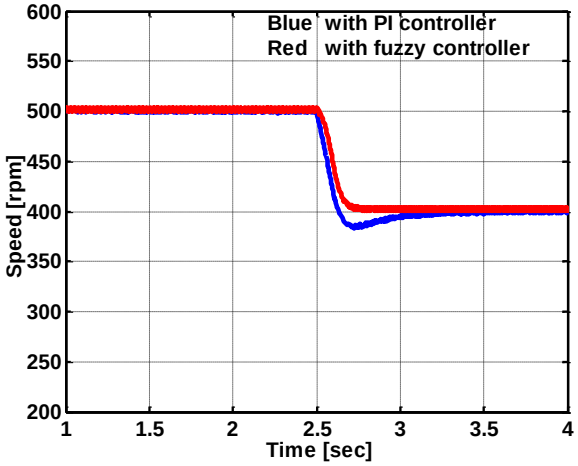

Figure.17 Comparison of the motor speed with negative change in reference speed for PI and FLPI controllers.

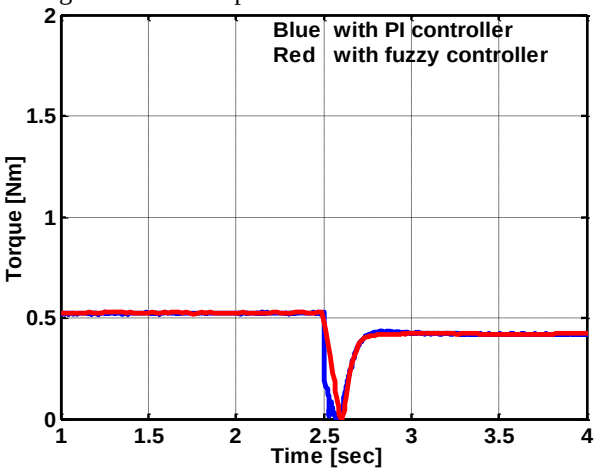

Figure.18 Comparison of the developed torque with negative change in reference speed for PI and FLPI controllers.

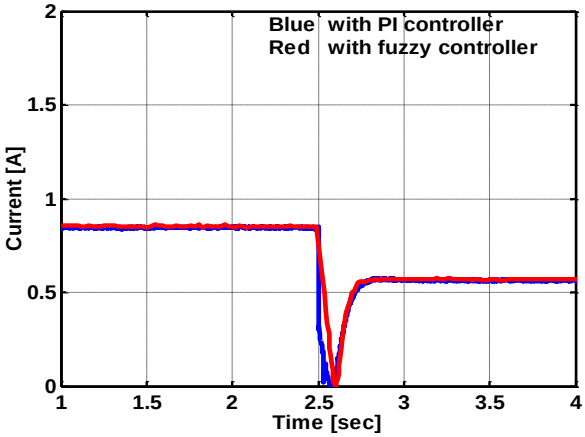

Figure.19 Comparison of the dc link current with negative change in reference speed for PI and FLPI controllers.

4.3. Load change

The proposed adaptive FLPI controller is tested under sudden load change in comparison with PI controller. Figures 20, 21 and 22 show the torque, current and speed responses for step increase in the load torque from 0.4 N.m to 0.8 N.m at a time 2.5 sec.

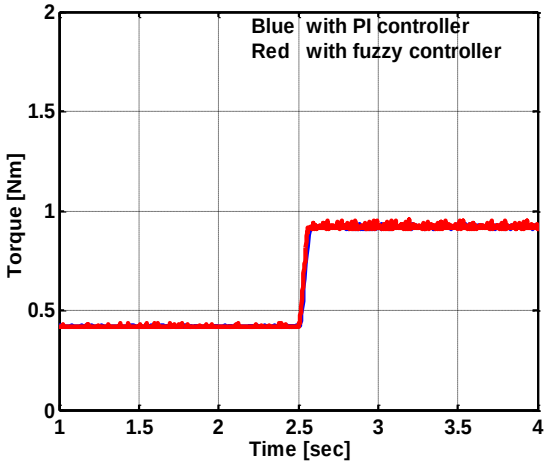

Figure.20 Comparison of the developed torque with positive load change for PI and FLPI controllers.

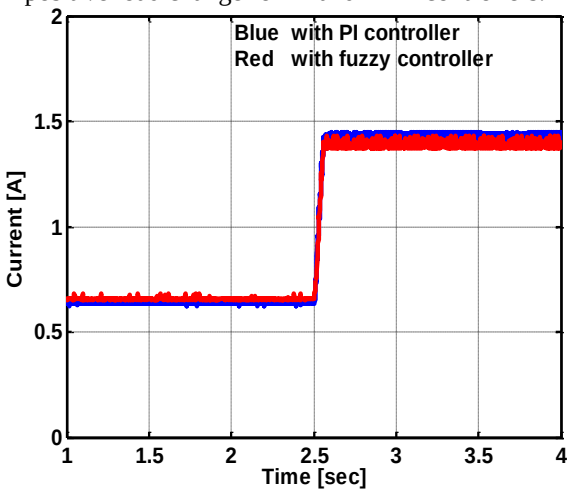

Figure.21 Comparison of the dc link current with positive load change for PI and FLPI controllers.

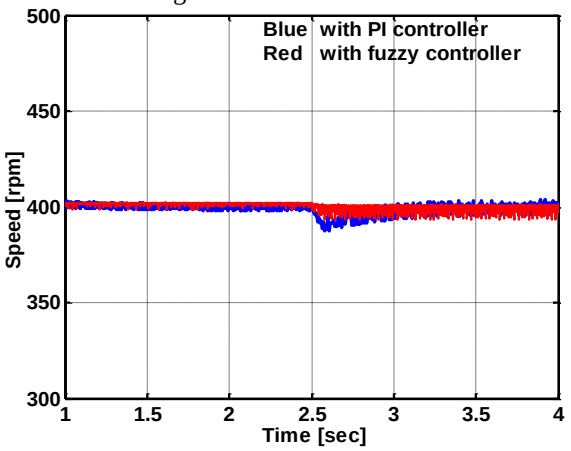

Figure.22 Comparison of the motor speed with positive load change for PI and FLPI controllers.

It is clear that the proposed controller has a faster speed response as shown in Fig.21. The test is repeated under sudden load decrease from 0.8 N.m to 0.4 N.m at time 2.5 sec and the results shown in figures 23, 24, and 25. The motor response obtained from this test assures the superiority of the proposed adaptive FLPI controller

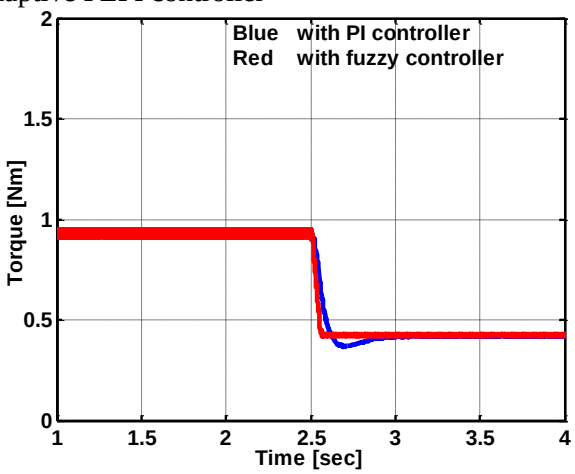

Figure.23 Comparison of the developed torque with negative load change for PI and FLPI controllers.

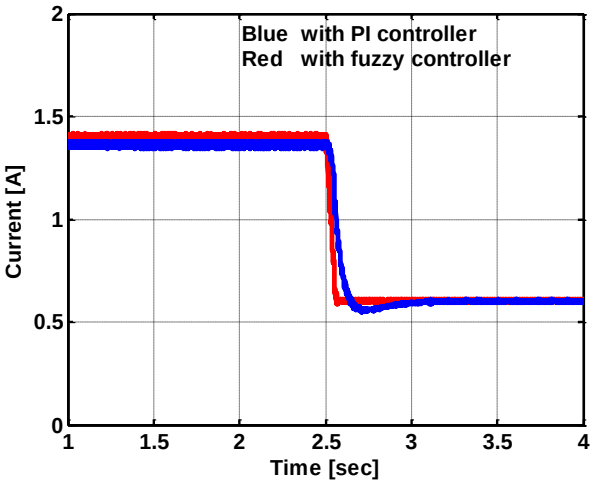

Figure.24 Comparison of the dc link current with negative load change for PI and FLPI controllers.

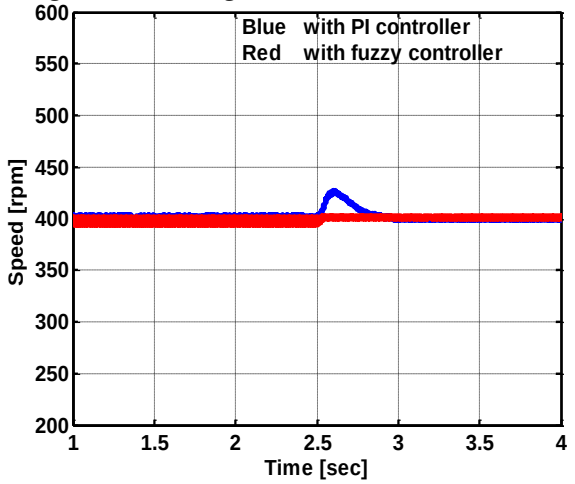

Figure.25 Comparison of the motor speed with negative load change for PI and FLPI controllers.

5. Conclusion

In this paper, both adaptive fuzzy logic PI controller and traditional PI controller are applied to an SRM represented by a simple nonlinear mathematical model.

The phase inductance has been predicated from finite element analysis and a simple nonlinear model has been devised to represent it as a function of phase current and rotor position. The results show that the characteristics obtained from this model are comparable with those based on FEA. This model has been used to represent the motor incorporated into the proposed two types of control techniques.

The comparison between two controllers performance has been carried out at motor starting as well as speed and load changes. The results show that the fuzzy logic modifier reduces the overshoot in the speed, torque and current responses in the most operating conditions. It has been also shown that the adaptive fuzzy logic PI controller has a fast response compared to traditional PI controller. These results assure the validity and accuracy of the proposed inductance model to represent the SRM for control purposes. So, the nonlinear inductance model proposed in this article may also be used effectively with other control systems.

References

[1] T. Miller," Optimal Design of Switched Reluctance Motors", *IEEE Transactions on Industrial Electronics*, Vol. 49, No. 1, pp.15-27, February 2002.

[2] J. Choi, S. Kim, Y. Kim, S. Lee and J. Lee, "Multi-Object Optimization of the Switched Reluctance Motor", *KIEE International Transactions on EMECS*, Vol. 4-B No. 4, pp.184-189, 2004.

[3] I. Husain, and S. Hossain, " Modeling, Simulation, and Control of Switched Reluctance Motor Drives", *IEEE Transactions on Industrial Electronics*, Vol. 52, No. 6, pp.1625-1634, December 2005.

[4] I. Kioskeridis, and C. Mademlis," Maximum Efficiency in Single-Pulse Controlled Switched Reluctance Motor Drives" *IEEE Transactions on Energy Conversion*, Vol., 20, No. 4, pp.809-817, December 2005.

[5] R. Inderka, and R. Doncker, "High-Dynamic Direct Average Torque Control for Switched Reluctance Drives", *IEEE Transactions on Industry Applications*, VOL. 39, NO. 4, pp.1040-1045, July/August 2003.

[6] F. Raj, V. Kamaraj,"Neural Network Based Control for Switched Reluctance Motor Drive", *IEEE International Conference on Emerging Trends in Computing, Communication and Nanotechnology (ICECCN)*, pp.678-682, 2013.

[7] A. Cheok and Y. Fukuda,"A New Torque and Flux Control Method for Switched Reluctance Motor Drives", *IEEE Transactions on Power Electronics*, Vol. 17, No. 4, pp.543-556, July 2002.

[8] R. Inderka, M. Menner, and R. Doncker," Control of Switched Reluctance Drives for Electric Vehicle Applications" *IEEE Transactions On Industrial Electronics*, Vol. 49, No. 1, pp.48-53 February 2002.

[9] S. Sahoo, S. Panda, and J. Xu," Indirect Torque Control of Switched Reluctance Motors Using Iterative Learning Control", *IEEE Transactions On Power Electronics*, Vol. 20, No. 1, pp.200-208, January 2005.

[10] S. Schulz, and K. Rahman, "High-Performance Digital PI Current Regulator for EV Switched Reluctance Motor Drives", *IEEE Transactions on Industry Applications*, Vol. 39, No. 4, pp.1118-1126, July/August 2003.

[11] C. Li, G. Wang, Y. Fan, Y. Bai, "A self-tuning fuzzy PID speed control strategy for switched reluctance motor", *Chines Control and Decision Conference (CCDC)*, pp 3084-3089, 2016.

[12] C. Liu, Y. Huo, X. Zhang, J. Liu, H. Chen," Fuzzy Embed into PI Control Algorithm of Switched Reluctance Motor", *IEEE International Conference on Information and Automation*, pp. 505-509, 2013.

[13] A. Tahour, A. Aissaoui, A. Megherbi," Fuzzy PI control through optimization: A new method for PI control of switched reluctance motor", *IEEE International Conference on Complex System*, pp. 1-7, 2012.

[14] F. Salmasi and B. Fahimi, "Modeling Switched-Reluctance Machines by Decomposition of Double Magnetic Saliencies", *IEEE Transactions on Magnetics*, Vol. 40, No. 3, pp.1556-1561, May 2004.

[15] V. Cic´ and S. Vukosavic,"A Simple Nonlinear Model of the Switched Reluctance Motor", *IEEE Transactions on Energy Conversion*, Vol. 15, No. 4, pp. 395-400, December 2000.

[16] S. Hossain, and I. Husain, "A Geometry Based Simplified Analytical Model of Switched Reluctance Machines for Real-Time Controller Implementation" *IEEE Transactions on Power Electronics*, Vol. 18, No. 6, pp. 1384-1389, November 2003.

[17] N. Radimov, N. Hail, and R. Rabinovici, "Simple Model of Switched-Reluctance Machine Based Only on Aligned and Unaligned Position

Data" *IEEE Transactions on Magnetics*, Vol. 40, No. 3, pp. 1562-1572. May 2004.

[18] M. Khater, H. Abdel-Maksoud, and S. El-Doheimy, "Performance of Three-Phase Switched Reluctance Motors with Different Structures: Comparative Study", *10th International Middle East Power Systems Conference (MEPCON)*, pp. 239-245, December, 2005.

[19] H. Abdel-Maksoud, M. Khater, and A. Oshieba," A Simplified Nonlinear Model of Switched Reluctance Motor", *Engineering Research Journal*, Vol.29, No. 4, pp. 329-335, October 2008.